Role of Carbon Nanoparticles and Near Infrared Laser Radiation for Treatment of Subcutaneous Ehrlich Carcinoma Model

Mostafa Yahia Mostafa[1], Mahmoud S. Elbasiouny [2], Tarek Atta [2], Tarek F. Elwakil[2] , Mahmoud abdalaziz[2] , Omar Abdel Aziz[2] ,Mohamed A. Elsayed[2].

[1] Affiliation (Department of medical applications of lasers, national institute of laser enhanced science, Cairo University, Egypt); m.y.mostafa77@gmail.com .

Article History: Received: 15.05.2023 **Revised:** 19.06.2023 **Accepted:** 22.06.2023

ABSTRACT

According to the World Cancer Report 2008 issued by the World Health Organization, there were an estimated 12.4 million new cases of cancer worldwide in 2018 and 7.6 million deaths from the disease. The most widely used cancer treatment procedures are chemotherapy and radiation. The use of combined LASER&MWCNT therapy for the mice transplanted by Ehrlich solid carcinoma produced better results and was more effective than the single treatment with LASER alone; Achieving higher necrosis in the tumor cells which will lead to higher chances of recovery and healing.

Keywords: nanoparticles, MWCNT, hyperthermia, tumor bearing mice, near infrared laser.

INTRODUCTION

According to the World Cancer Report 2008 issued by the World Health Organization, there were an estimated 12.4 million new cases of cancer worldwide in 2018 and 7.6 million deaths from the disease [1]. The most widely used cancer treatment procedures are chemotherapy and radiation. Both techniques rely on damaging DNA of the cells, disrupts replication, inducing apoptosis or programed cell death [2]. Radiation therapy can provide a more target-specific treatment option when compared to chemotherapy. The limitation of radiation therapy is that normal tissue surrounding tumors is also damaged [3].Hyperthermia treatment is elevating tumor temperature above certain levels with sufficient heating duration. It has been proposed as an alternative to traditional cancer treatment options. It has been shown that elevating tumor temperature above 42°C causes cell death. Based on the different temperature ranges achieved, hyperthermia can be broadly classified into mild hyperthermia with a temperature range of 43°C, to ablation hyperthermia requiring a temperature range much higher than 49°C. Research in hyperthermia over the past three decades provides us with a good understanding of cytotoxicity dosing but it is difficult to deliver the thermal dose accurately [4]. Nanoparticle hyperthermia has attracted a lot of attention to effectively deliver heat to targeted tumor region while preserving the surrounding healthy tissue [5].

Nanotechnology, which is a multidisciplinary science involving chemistry, biochemistry, physics, and materials science, has found uses in a wide spectrum of medicine-related applications [6]. These include nanoparticle-based imaging, drug delivery, bio-sensoring, and hyperthermia, and in the past decade, a number of these nanoparticle-based techniques have been translated into clinical applications. Materials exhibit unique physical and biochemical properties when their dimensions are reduced to between several to hundreds of nanometers. A highly localized treatment can be achieved using magnetic nanoparticle hyperthermia as this technique only leads to heat generation in the areas that contain magnetic nanoparticles. Iron-based nanoparticles such as Fe3O4 and Fe2O3 are possible candidates for use in magnetic nanoparticle hyperthermia, due to their biocompatibility, their ability to produce high

temperatures, as well as their potential to confine the heating to the tumor [7]. Small concentrations of nanoparticles typically cause no toxic reaction from the body and they are typically secreted from the body by the spleen, the liver, and the lymphatic system [8].

Carbon nanotubes (CNTs), first discovered by Iijima in 1991[10], are made up of thin sheets of benzene ring carbons rolled up into the shape of a seamless tubular structure. This novel structure belongs to the family of fullerenes, the third allotropic form of carbon along with graphite and diamond. CNTs are generally produced by three major techniques: electric arc discharge, LASER ablation, and thermal or plasma enhanced chemical vapor deposition (CVD) [9]. Based on their structure, CNTs can be classified into two general categories: single walled (SWNTs), which consist of one layer of cylinder graphene and multi-walled (MWNTs), which contain several concentric graphene sheets [10]. CNTs have unique physical and chemical properties such as high aspect ratio, ultralight weight, high mechanical strength, high electrical conductivity, and high thermal conductivity etc. [11]. The combination of these characteristics makes CNT a unique nanomaterial with the potential for diverse applications, especially in biomedical field. [12]

Even for those patients who underwent radical resection of the tumor, radiochemotherapy and other treatments are sometimes recommended to prevent relapse caused by residual micro-metastases. Although these modalities are successful in some cases, systemic toxicity may develop at the same time due to lack of selectivity for these treatments [13]. The transporting capabilities of carbon nanotubes combined with appropriate surface modifications and their unique physicochemical properties can lead to a new kind of nanomaterials for cancer therapy At the same time, due to their remarkable physicochemical properties as mentioned above, CNTs are also welcomed in the field of thermal therapy and considered to be a non-invasive, harmless, and highly efficient technique [14].

Exposure to MWNTs in radiofrequency (RF) field would lead to significant heat release by. Both in vitro and in vivo tests have shown thermal destruction of cancer cells in the presence of SWNTs with exposure to radiofrequency field [15].

Carbon nanotubes have the ability to absorb near-infrared (NIR) radiation (700–1100 nm) and then convert it into heat, which provides an opportunity to open up new strategies for cancer thermal therapy [16].

Infrared photo thermal (PT) radiometry, combined with recent Advances in time-resolved infrared imaging techniques, was a very useful tool for determining the temperature dynamics in scattered individual cancer cells or their small clusters labelled with carbon nanotubes, which was helpful in determining the appropriate dose regimens for LASER PT therapy using relatively long LASER pulses. The investigators believe that the approach could be particularly useful for treating small tumors, tumor margins, and micro-metastases. In another work [17],

Moon and his group combined the treatment of SWNTs and NIR irradiation in nude mice bearing human epidermoid mouth carcinoma KB tumor cells on their backs. After intratumoral injection of PEG-SWNTs solution, the mice then received near infrared irradiation with a power density of 76 W/cm ^{3} for 3 min in the tumor region. The mice treated with PEG-SWNTs and NIR irradiation showed complete destruction of tumors after 20 days of post-treatments. Moreover, it is found that most of the injected SWNTs were almost completely excreted from mice bodies in about 2 months through biliary or urinary pathway. In a similar work, long-term survival of kidney-tumor-bearing mice was acquired via MWCNT-based treatment, but with low LASER powers (3 W/cm2) and very short treatment time (a single 30-sec treatment) [18].

In order to increase the selectivity of treatment and decrease toxic effects to normal cells, the targeting of CNTs to tumor cells for NIR mediated killing has been accomplished by both non covalently and covalently coating CNTs with cell-binding ligands such as

peptides or monoclonal antibodies (MAbs). However, these results mostly detected tumor cells in vitro rather than in vivo animal models. The efficiency of nanoparticle delivery to targeted sites using systemic delivery relies on coating of the nanoparticles specifically targeting cancer cells and adequate local blood perfusion rate in the tumors. On the other hand, direct injections of nanoparticles into tumors may be a better option to confine the nanoparticles into the targeted tumor region. Intratumoral injection of nanoparticles also has the advantage of targeting poorly perfused tumors. For a tumor with an irregular shape, multiple nanoparticle injection can be exploited to cover the entire tumor and therefore, resulting in a more uniform thermal damage to the tumors. Previous studies have tried to achieve uniform nanoparticle distribution in tumors with minimal success [19].

MATERIALS AND METHODS

ANIMALS AND TUMOR MODEL:

♦*Animals*

Female Swiss albino mice weighing 18-22 grams, (6-8) weeks old were selected. Animals were housed in suitable cages in a room with regular light /dark cycle, and were kept on pellet diet and water ad libitum.
Animal care was performed according to the standard regulations of experimental animals.

♦*Tumor model*

The tumor used in this study was a solid Ehrlich carcinoma which is a transplantable, poorly differentiated malignant tumor which appeared originally as a spontaneous breast carcinoma in a mouse. It grows in both solid and ascitic forms.
A line of Ehrlich ascites Carcinoma (EAC) was supplied from the breading unit of the National Cancer Institute, Cairo University. In this study 1×106 (EAC) cells, single cell suspension were transplanted by subcutaneous inoculation in the mice dorsum using a moderate rate of injection to avoid dispersion flow of the inoculum and to obtain a single grafted tumor.
The tumors developed within seven days after injection, and animals with tumor dimensions in a range of (8-10mm) in its largest diameter and a thickness range of (3-5mm) were selected to be used in this study. The volumes of these tumors range from 119.8 to130.5 mm3.
The day before irradiation the skin overlaying the tumor in the mice was depilated by means of cream (Veet, England). This time interval before irradiation was required to avoid the bias of phototherapeutic studies by the presence of allergic or inflammatory reactions at the level of the treated skin.

EXPERIMENTAL:

Materials and chemicals:

Multi-tubes Carbon nanotube MCNTs was synthesized using materials and chemicals characterized and listed in the table (1).

Table 1: the main Characteristics of the chemicals and material used in the synthesis of MWCNTS

name	type	source	Melting Point ˚C	Boiling point ˚C	Chemical form	Density g/cm^3	Act as
Toluene	Colorless liquid	Fisher Scientific, UK	-95	110-111	C_7H_8	0.87 at 25°C	Carbon precursor

Ferrocene	Light orange powder	Sigma-Aldrich, UK	173	249	$C_{10}H_{10}Fe$	1.49 At 25°C	Carbon precursor, Catalyst donor

Synthesis of MWCNTs experimental procedure.

The injection chemical vapor deposition (InJ-CVD) method was employed to synthesize MWCNTs [21-23] in a typical experiment setup as shown in (figure 1). The main tubular furnace temperature, synthesizing pyrolysis temperature, was 700 ± 5 °C under the flow of 100 cc/hr of argon (pyrolysis medium as well as carrier gas) at atmospheric pressure. The volume of carbon source (Toluene) and catalyst (Ferrocene) was adjusted to 5% (w/w) weight percentage respectively. The feed solution was injected uniformly with 2.21 cc/h by using syringe pump to a preheated tube which put in horizontally position at a temperature of 200°C for 1 hr.

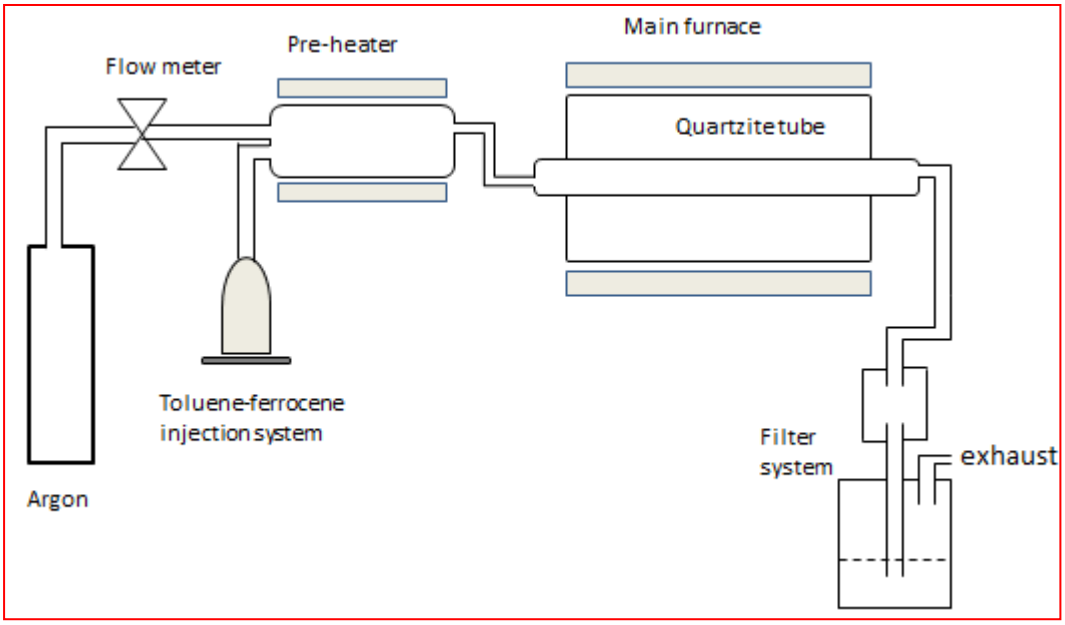

Fig 1. Schematic diagram of Injection CVD setup

Characterizations of synthesized MWCNTs:

The quality of MWCNTs is investigated by the Raman spectra. The result was recorded in the range of 550 – 3500 cm^{-1} with a 12.5 nm power and a 532 nm laser excitation line. On the other hand the purity and the thermal stability of the syntheses sample were studied by Thermal Gravimetric Analysis (TA55).

HYPERTHERMIA TREATMENT STUDIES:

• *Source for hyperthermia treatment:*

LASER system [G-box medical diode laser systems Giga laser] its wavelength was 980 nm, and it is a CW LASER having an output power range from 1 to 15W that can be adjusted in 0.5W increments and it has a red aiming beam. LASER energy was delivered to the lesion through flexible fiberoptic 400 μm in diameter.

• *Hyperthermia treatment procedures:*

A LASER power of 1W was used in these experiments as follows:

First: continuous application of LASER energy to the tumor to reach the required temperature whether (42°C or 44°C).

Second: maintaining this temperature by on / off the LASER beam according to the temperature measurements for a period of 10 minutes.

EXPERIMENTAL DESIGN:

32 *Female Swiss albino mice weighing 18-22 grams* was divided in 4 groups each having 8 mice as following:

Control group which received no treatment

Laser only group

MWCNT group

LASER+MWCNT group

ASSESSMENT OF THE TREATMENTS RESPONSES

Morphological Assessment

A-Macroscopic study:

Responses of the tumor and overlying skin to the different treatment schedules were followed daily for 21days after treatment. The changes that occurred in the tumors after treatment were described considering the shape and duration of these changes. The number of mice affected by a change per group were also determined.

B- Microscopic Study

1-Histopathology:

Specimens were taken after animal sacrifice by exposure to ether vapor at: 24 hours, 7 days, 14 days and 21days after treatment.

Tumor specimens were excised and fixed in 10% formalin solution, processed by routine paraffin technique; step serial histological sections were prepared from the paraffin blocks and stained with hematoxylin and eosin. Histological picture of the specimens were described.

2-Necrosis percent:

The specimens taken at, 24 hours and 7days after treatment were subjected to another semi-quantitative measurement of the necrotic areas that was performed by projecting the microscopic image to a television screen by a video camera attached to the microscope; a translucent paper divided in large number of equal squares was fixed to the television screen. This was repeated in at least five-step section for each paraffin block. So, the necrotic surface area in the microscopic section could be compared to the intact area of the tumor of the same section.

II.TUMOR GROWTH

1-Tumor volume:

After the treatment, tumor diameters were documented three times a week by Vernier caliper measurements in three orthogonal diameters (D_1, D_2, and D_3) where D_1 is the longest diameter, D_2 is the shorter diameter, and D_3 is the height. Tumor volume was calculated by the equation

$$V = (\pi/6)(D_1 \times D_2 \times D_3).$$

These measurements were achieved to all animal groups for 21 days after treatment. The changes in volume of the tumors as affected by different treatment schedules presented as a mean ±SD and shown in tables and graphically represented as growth curves for experimental and control groups.

2-Tumor growth inhibition ratio (TGIR):

The inhibition of tumor growth rate when compared to untreated group was determined by the equation ($V_c - V_t$) / V_c x 100 %) where V_c is volume of untreated group V_t is the volume of treated groups of mice respectively. This calculations where done for the measurements taken at days (7, 14, 21) post treatment and presented as a mean ±SD.

3-. SURVIVAL PERIOD:

All animals were housed in similar environmental conditions and received the same diet. In this study the number of animals surviving in each group to the end of 90 days was thus consequently considered to be the impact of the treatment modality on animal's life. The number of mice deaths will be recorded every 10 days and notes will be taken on decline in the number of the mice along the follow up period the data presented in charts.

STATISTICAL METHODS:

Quantitative data were tested for normality of distribution using Kolmogorov Smimov test. Normally distributed data were summarized as means and standard deviations. Group means were compared by Student t-test if they were two groups or by one-way analysis of variance (ANOVA) test if more than two. A significant ANOVA was followed by Tukey honestly significant difference test (HSD) to show which pairs of groups differ at 5% probability level. The data were represented graphically.

Non-normal data were summarized as 25th, 50th (median) and 75th percentiles and compared using Mann-Whitney U test (if 2 groups) or using Kruskal Wallis test (if more than 2).

Qualitative data were compared by Chi-square or Fisher's exact test according to the expected frequencies.

A 5% probability level ($p>0.05$) was considered statistically non-significant, ($p<0.05$) significant, and $p<0.0l$ or less highly significant.

Calculations were done on the Statistical Package for Social Science (SPSS) programme, version 6.

Results and Discussion

Quality investigation:

Generally, the type and quality of MWCNTs was detected by the Raman spectroscopy technique. CNTs with all of its types were identified by three main Raman peaks [26]. Which called D, G and 2D bands, which produce at Raman shift around 1350, 1500 and 2700 cm^{-1} respectively. Figure (2) shows the Raman spectra for the prepared MWCNTs at 700 °C synthesizing temperature. Raman spectra not only used to differentiated the types of CNTs as SWCNTs, DWCNTs or MWCNTs but also can be used to measure the quality of the prepared sample [25]. The quality of MWCNTs was investigated by dividing the intensity (Full wigth half maximum) of the disordered peak (ID) over the intensity (FWHM) of the graphitization peak (IG) [27]. MWCNTs were recorded below 0.3 aspect ratio ID /IG [24] as shown in (figure 2) which mean high quality MWCNTs.

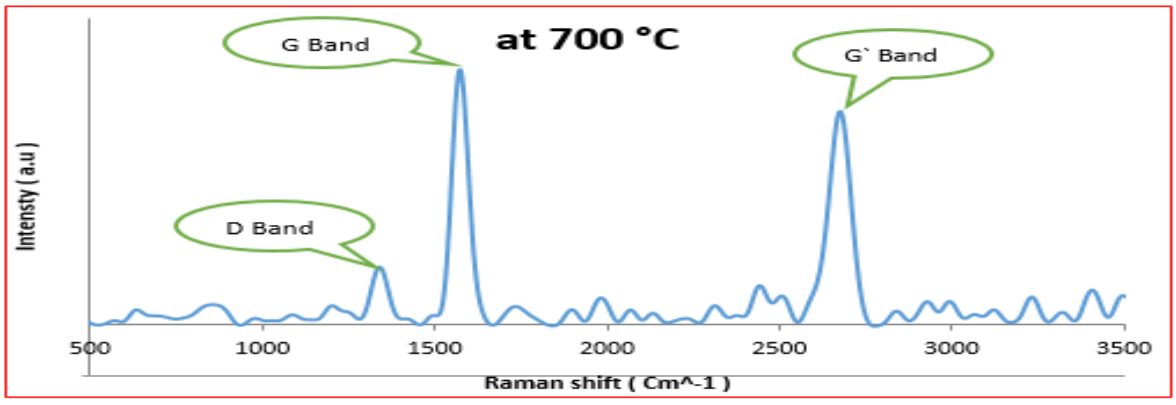

Fig 2 Raman spectra for the prepared CNMs at 700 ˚C pyrolysis temperature, by injection solution of 5%Wt Ferrocene in Toluene under 100 cc/h argon atmosphere for 1 hr.

Morphology and average outer diameter investigation:

A scanning electron microscope (SEM) is a sensitive technique to illustration the material morphology and estimate the average outer diameter of prepared MWCNTs. Figure B shows the SEM image of MWCNTs sample synthesized at 700 ˚C pyrolysis temperatures, the average outer diameter was 35±10 nm.

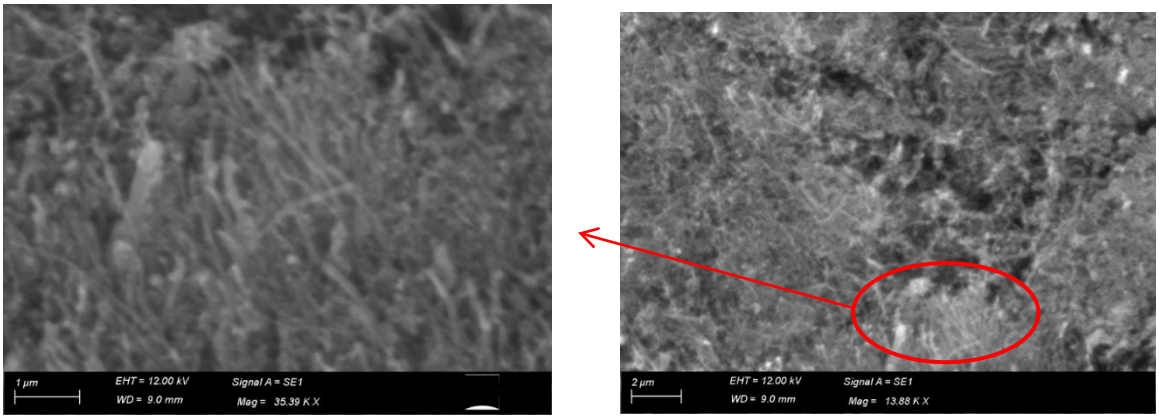

Fig 3 SEM images of MWCNTs samples synthesized at 700˚C pyrolysis temperatures with different scale bar and different magnifications

Evaluation of dimensions of high-quality samples using (HITEM):

High-resolution transmission electron microscope (HITEM) using to characterize the outer and inner diameter and calculate the number of tubes for MWCNTs. Here HITEM used especially to confirm that the sample synthesized at 700˚C, which had average ID/IG aspect ratio lower than 0.3, is MWCNTs as shown in (figure a). The averages of outer and inner diameter were 26±9 nm and 7.9 ± 1.8 nm respectively, as shown in (figure 7b). Because of the inner spacing between tunes around 0.36nm [23,29], the average number of tubes for this high-quality MWCNTs was 23±7 tube. The dark spots in both figures 4(a, b) were the iron metal catalyst.

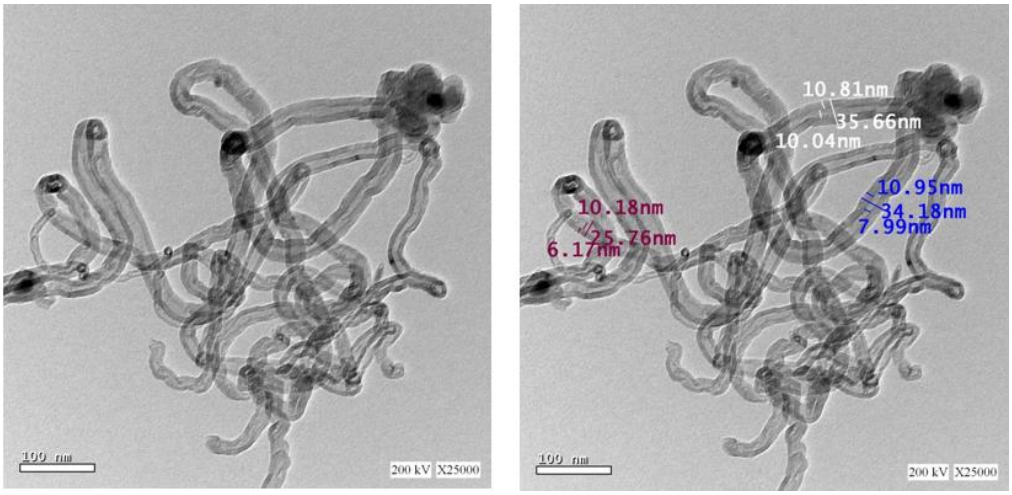

Fig 4 HITEM of MWCNTs at 700˚C with Mag=25XK (a) without diameters information and (b) with outer and inner diameters.

Thermal Oxidation Stability of MWCNTs study by TGA:

In this part of the work, not only the thermal stability of syntheses MWCNTs was studied but also the purity was calculated by using Thermal Gravimetric Analysis (TGA)[30]. It has been known that the oxidation temperatures for amorphous carbon contaminants, SWCNTs, and MWCNTs are typically in the range of 200 – 300 °C, 350 – 500 °C and 400–650 °C respectively [31,32]. Figure 00 shows the thermos-gram for MWCNTs synthesized at 700 °C pyrolysis temperatures. The results revealed that in the temperature range from 200˚C to 400˚C very low weight loss was observed. This could be attributed to the prepared samples are free of amorphous carbon. Figure 00 shows that the oxidation temperature around 591˚C, for the sample prepared at synthesizing temperature of 700 ˚C.

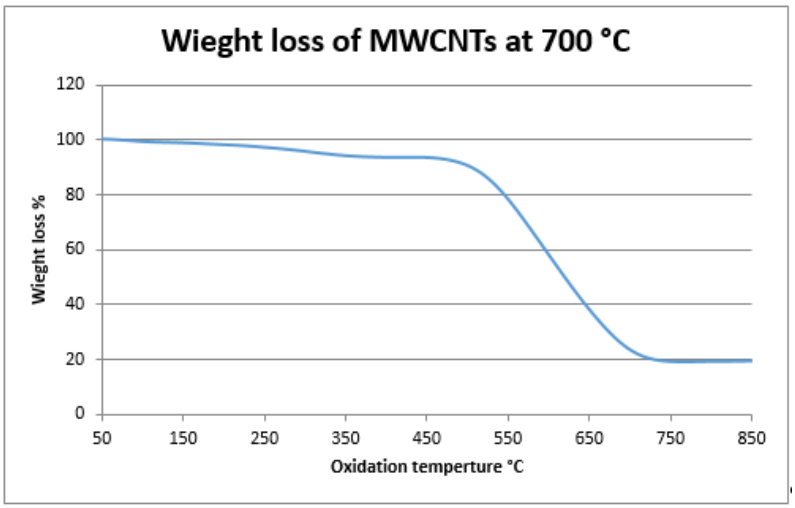

Fig 5 Thermo-gram for MWCNTs at 700˚C, pyrolysis temperature

• *Results of Temperature measurements:*

In HPT treatment groups: The mean time to reach treatment temperature at 44 °C during interstitial HPT was 2.6 minutes while combined LASER and MWCNT was 0.29 minutes as shown in the graph below.

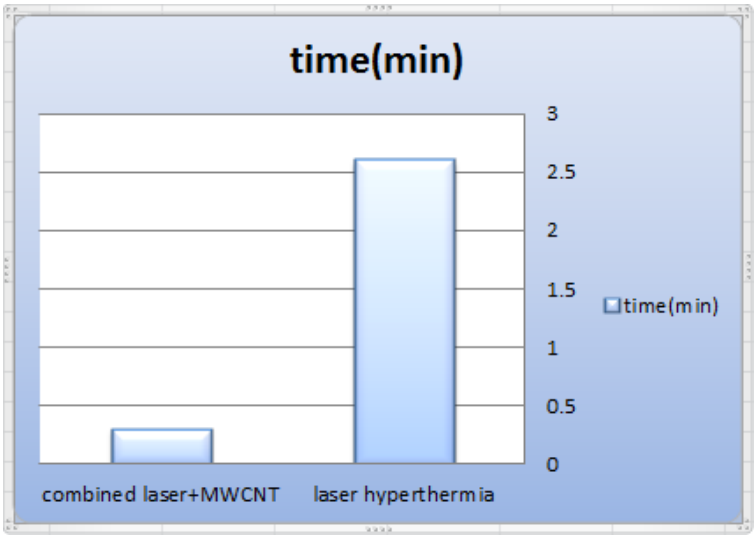

Fig 6 the mean time to reach mean temperature

III- RESULTS of tumor morphological changes

♦*Control Group*

Before treatment had started the tumors from all groups was ellipsoid in shape with regular contour, more or less flattened under surface and firm consistence. The overlaying skin presented neither special adhesions nor abnormal vascularity.

The Ehrlich carcinoma tumor cells transplanted subcutaneously in the mice and reached a volume range of 119.8-130.5mm3, within 7-8 days after transplantation (the day of starting treatment in the other groups). Tumors continued to grow and reached a volume range of 1.260-1.504 mm3 after 21 days the tumor was a cauliflower like at that time with no special skin signs.

Fig 7 Shows the difference in tumor size between the control group at the beginning of treatment (right) and 21 days later (left).

The LASER Hyperthermia Group showed edema and hyperemia in all the treated tumors and in a small zone of its surrounding normal tissue started 30-45 min. and lasted during the first 24 hours after treatment. It occurred in all the tumors of these two treatment groups which treated with either 42°C or 44°C.

Fig 8 showing after the treatment with LASER hyper thermia.

Macro of combined LASER&MWCNT group

Fig 9 after treatment with combined LASER&MWCNT

- RESULTS OF SURVIVAL PERIODS STUDY:

As all the mice were incubated in the same similar environmental conditions and received the same diet, so the number of mice surviving from each group during the next 80 days after tumor implantation was considered as an index about the effectiveness of treatment modality. Then the pattern of mice death will be presented according to the decline in number along the follow up period.

The results of survival periods arranged from the shorter survival periods to the longer periods are shown in the Table below

Groups	SURVIVAL PERIOD [Days]
1. Control group	32
2. Laser only group	47
3. MWCNT group	66
4. LASER+MWCNT group	84

Table 2 showing survival periods for all groups

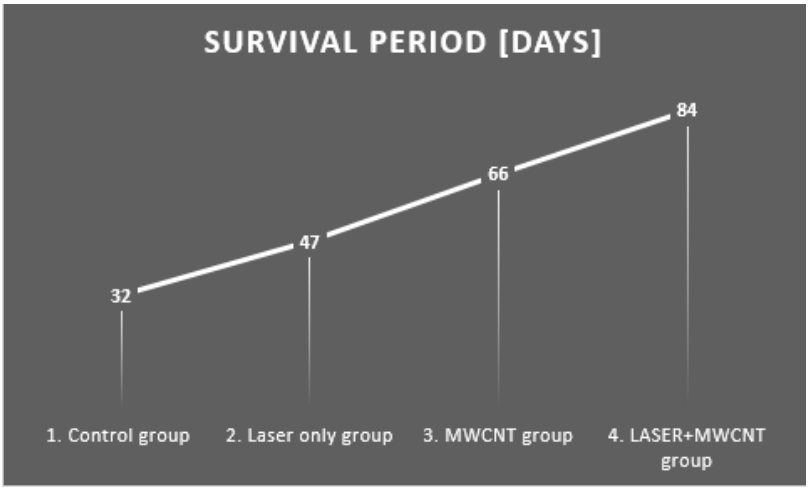

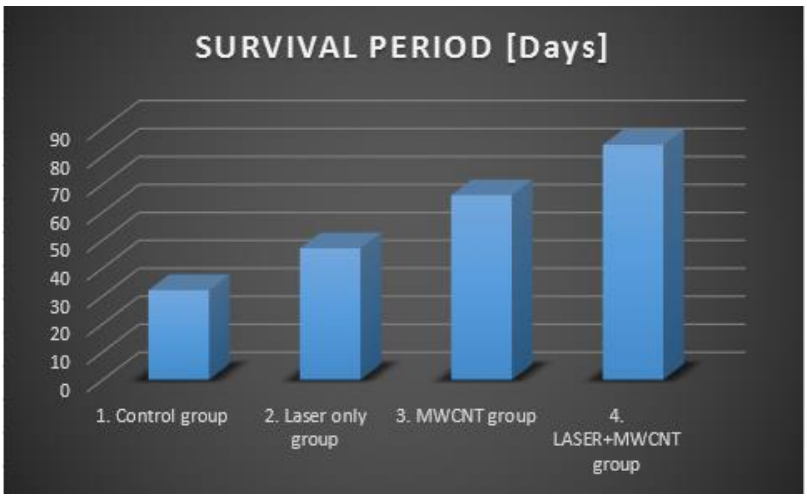

Figure 10, 11 showing the survival periods of all groups

Tumor growth inhibition ratio (TGIR):

Tumor growth inhibition ratio presented as a mean percent (±SD) calculated for each tumor in all the treatment groups at (7, 14, 21 days) after starting the treatment. As the following Table:

Mean TGIR % of the Treatment Groups	7 days after starting	14 day after starting	21 days after Starting
Laser only group	40.3	53.1	62
MWCNT group	57.6	64.9	75.4
LASER+MWCNT group	87.2	96.1	97.9

Table 3 showing the mean TGIR % for treated groups

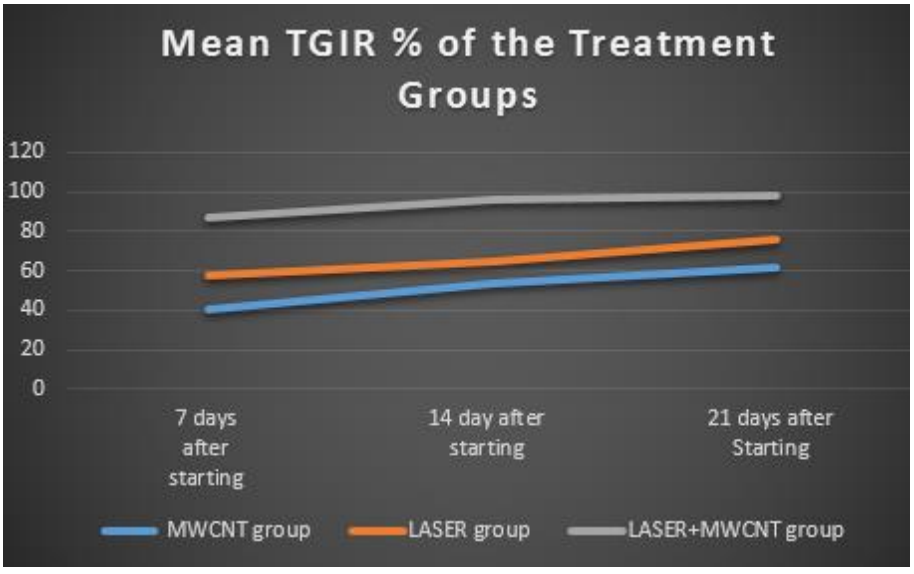

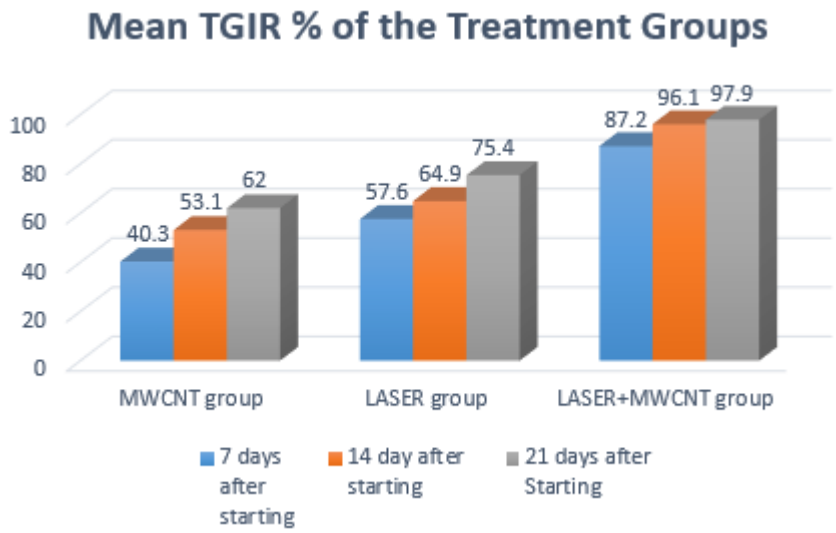

Figure 12, 13 showing the mean tumor growth inhibition ratio percentage for treated groups

Results of Tumor volume changes:

Measurements of the tumor volumes in all the study groups will be presented as a mean (±SD) for each group along the follow up period at 7, 14, and 21 days from the starting day of treatment.as the following Table:

Volume Changes in (mm^3)	start of treatment	7 days after starting	14 day after starting	21 days after Starting
1. Control group	128.5	381	687	1268
2. Laser only group	129.8	173.2	279	449
3. MWCNT group	129.1	166.3	241.5	324.2
4. LASER+MWCNT group	125.5	52.3	29.6	21.4

Table 4 showing Volume Changes in (mm^3) along the follow up period

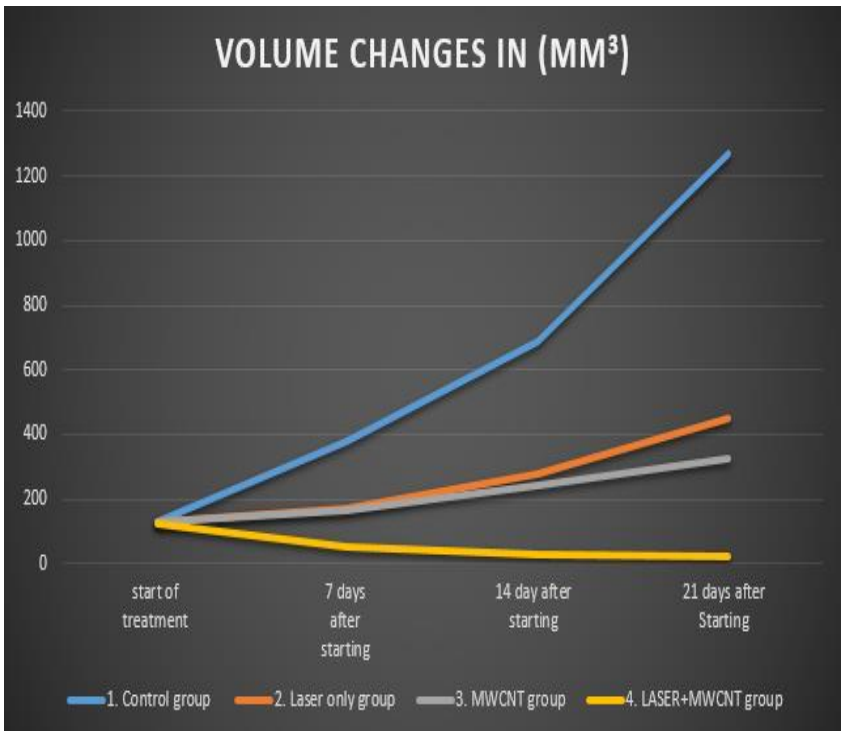

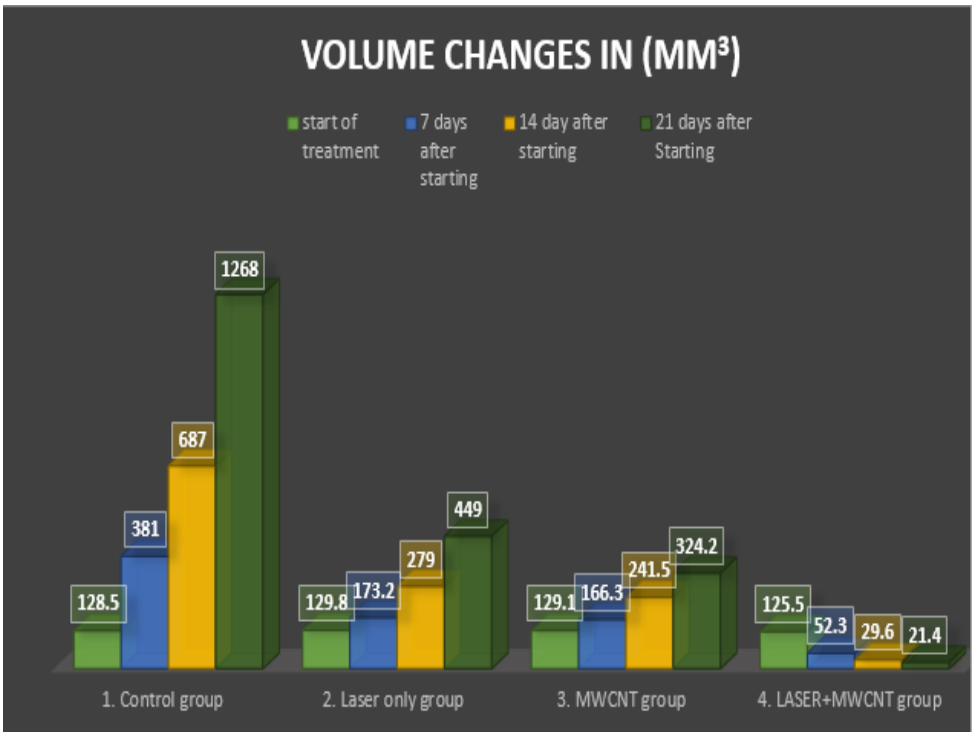

Fig 14, 15 showing Volume Changes in (mm^3) along the follow up period

MICROSCOPIC STUDY RESULTS

1. Histopathological result:

♦*Control group:*

Light microscopic examination of control group showed sheets of highly pleomorphic malignant tumor cells with hyperchromatic and pleomorphic nuclei and scant eosinophilic cytoplasm. Cells were arranged in sheets that vary in size and shape.

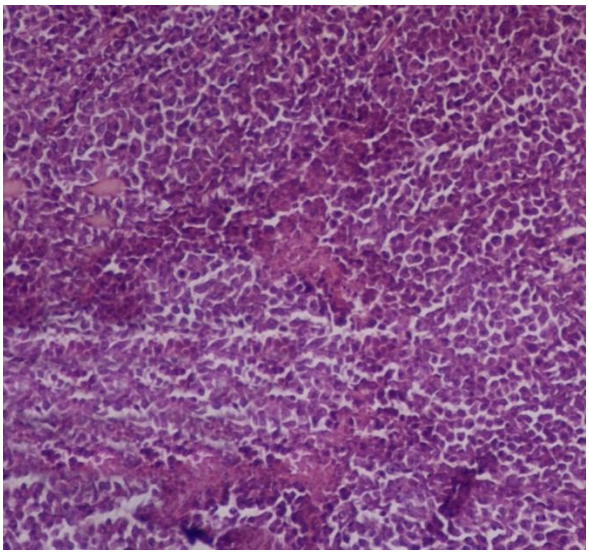

Fig 16 showing control group histology under [40X]

♦*The hyperthermic therapy group:*

Examination of solid Ehrlich carcinoma samples treated by hyperthermia showed more extensive edema and extravasations of erythrocytes and more areas of degeneration in the depth of the sample the effect of surface hyperthermia in the form of coagulative necrosis was more apparent in the superficial parts of tumor samples

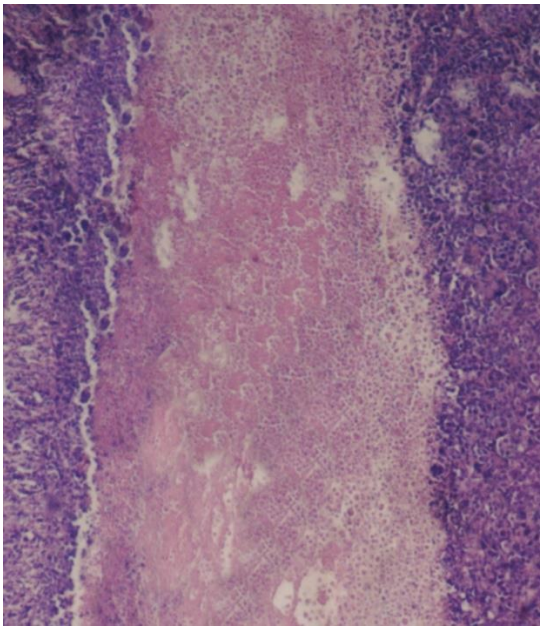

Fig 1*7* Photomicrograph of a histological section from Ehrlich carcinoma tumor of the interstitial

HPT group showed more necrosis in the central area

♦*The combined LASER and MWCNTS therapy group:*

Examination of solid Ehrlich carcinoma treated by combined LASER and MWCNTS showed that the effect of treatment efficacy of the treatment is increased with an observed increase in amount of tumor damage and a higher success rate of 96%.

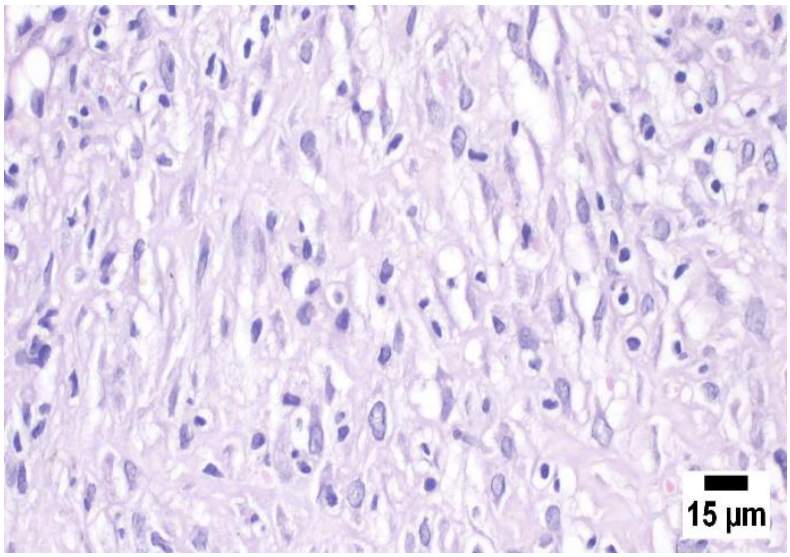

Fig 18 Photomicrograph of muscle, showing marked decrease of neoplastic cells with abundant collagenous matrix and reactive fibroblast (H&E).

2. Necrosis assessment

The necrotic surface area was compared to the non-necrotic tumor surface area and expressed as the necrosis present. This necrosis percent reflects approximately the effeteness of treatment modality. It was calculated in each specimen in all the treatment groups one and 7 days after treatment.

The results of necrosis percent after microscopic examination of the specimens as shown in the Table 5.

GROUP	Necrosis Percent, One day After Treatment	Necrosis Percent, 7 Days After Treatment	P value
Surface hyperthermia 42°C	30.1± 0.2 %	52.17 ± 4.3%	(P<0.05)
Surface hyperthermia 44°C	34.7 ± 1.5%	65.63 ± 18%	(P<0.05)
Combined LASER&MWCNT	51.8 ± 1.3%	92 ±4.7%	(P<0.05)

Table 5 showing the results of necrosis percent after microscopic examination of the specimens

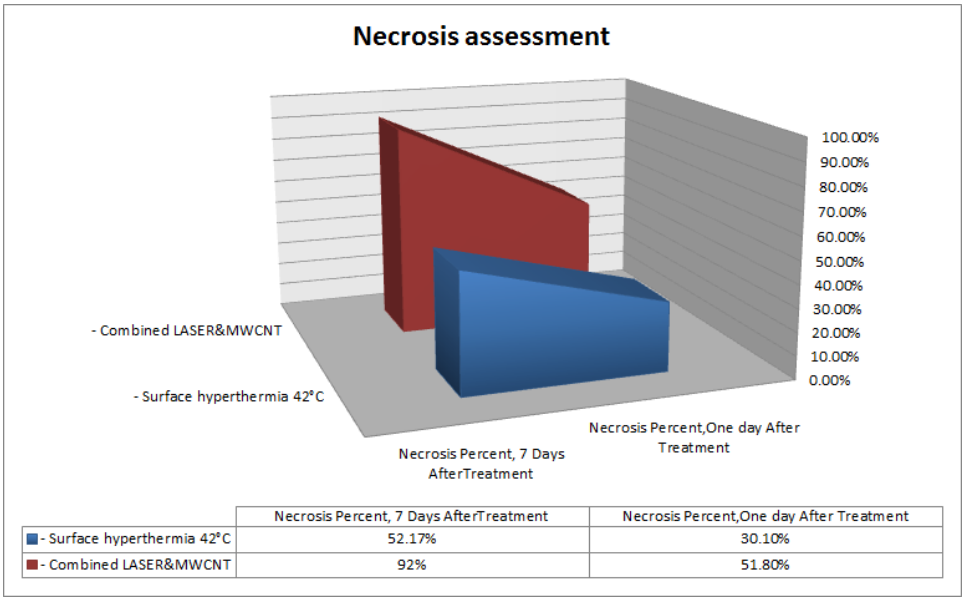

	Necrosis Percent, 7 Days AfterTreatment	Necrosis Percent,One day After Treatment
- Surface hyperthermia 42°C	52.17%	30.10%
- Combined LASER&MWCNT	92%	51.80%

Fig 19 showing the results of necrosis percent after microscopic examination of the specimens

CONCLUSIONS

This is an experimental study, we can conclude that: the use of combined LASER&MWCNT therapy for the mice transplanted by Ehrlich solid carcinoma produced better results and was more effective than the single treatment with LASER alone; Achieving higher necrosis in the tumor cells which will lead to higher chances of recovery and healing.

Author Contributions: A short paragraph specifying their individual contributions must be provided for research articles with several authors. The following statements should be used "Conceptualization, Mahmoud Sabry Elbsiony; methodology, Tarek Atta , Mahmoud Sabry Elbsiony.; validation, Tarek Fahmy Elwakil..; formal analysis, investigation and resources Mostafa Yahia , Omar Abdel Aziz[2] ,Mohamed A. Elsayed ; writing—original draft preparation, Mostafa Yahia.; writing—review and editing, Mostafa Yahia , Omar Abdel Aziz[2].; visualization and supervision, Tarek Fahmy Elwakil., Tarek Atta ,Mostafa Yahia.; project administration, Tarek Fahmy Elwakil,.; funding acquisition, Mostafa Yahia, Mahmoud abdalaziz[2]. All authors have read and agreed to the published version of the manuscript.

Funding: This research received no external funding.

Institutional Review Board Statement: In this section, please add the Institutional Review Board Statement and approval number for studies involving humans or animals. Please note that the Editorial Office might ask you for further information. Please add, "The study was conducted according to the guidelines of the Declaration of Helsinki and approved by the Institutional Review Board (or Ethics Committee) of NAME OF INSTITUTE (protocol code XXX and date of approval)." OR "Ethical review and approval were waived for this study due to REASON (please provide a detailed justification)." OR "Not applicable." for studies not involving humans or animals. You might exclude this statement if the study did not include humans or animals.

Acknowledgments: I would like to express my gratitude to my supervisors, Dr Mahmoud Saber, Dr Tarek Atta , Dr Tarek F. Elwakil and Dr Mahmoud Abdelaziz who guided me throughout this research. I would also like to thank my friends and family who supported me.

Conflicts of Interest: The authors declare no conflict of interest.

REFERENCES

1] Ferlay J, Colombet M, Soerjomataram I, Mathers C, Parkin DM, Piñeros M, Znaor A, Bray F. Estimating the

global cancer incidence and mortality in 2018: GLOBOCAN sources and methods. International journal of cancer. 2019 Apr 15;144(8):1941-53.

2] Huang R, Zhou PK. DNA damage repair: Historical perspectives, mechanistic pathways and clinical translation for targeted cancer therapy. Signal Transduction and Targeted Therapy. 2021 Jul 9;6(1):254.

3] Dunne M, Regenold M, Allen C. Hyperthermia can alter tumor physiology and improve chemo-and radio-therapy efficacy. Advanced Drug Delivery Reviews. 2020 Jan 1;163:98-124.

4] Kok HP, Cressman EN, Ceelen W, Brace CL, Ivkov R, Grüll H, Ter Haar G, Wust P, Crezee J. Heating technology for malignant tumors: A review. International Journal of Hyperthermia. 2020 Jan 1;37(1):711-41.

5] Alamdari SG, Amini M, Jalilzadeh N, Baradaran B, Mohammadzadeh R, Mokhtarzadeh A, Oroojalian F. Recent advances in nanoparticle-based photothermal therapy for breast cancer. Journal of Controlled Release. 2022 Sep 1;349:269-303.

6] Hardy JG, Sdepanian S, Stowell AF, Aljohani AD, Allen MJ, Anwar A, Barton D, Baum JV, Bird D, Blaney A, Brewster L. Potential for chemistry in multidisciplinary, interdisciplinary, and transdisciplinary teaching activities in higher education. Journal of Chemical Education. 2021 Mar 4;98(4):1124-45.

7] Joshi R, Singh BP, Ningthoujam RS. Confirmation of highly stable 10 nm sized Fe3O4 nanoparticle formation at room temperature and understanding of heat-generation under AC magnetic fields for potential application in hyperthermia. AIP Advances. 2020 Oct 1;10(10):105033.

8] Truskewycz A, Yin H, Halberg N, Lai DT, Ball AS, Truong VK, Rybicka AM, Cole I. Carbon dot therapeutic platforms: administration, distribution, metabolism, excretion, toxicity, and therapeutic potential. Small. 2022 Apr;18(16):2106342.

9] Rathinavel S, Priyadharshini K, Panda D. A review on carbon nanotube: An overview of synthesis, properties, functionalization, characterization, and the application. Materials Science and Engineering: B. 2021 Jun 1;268:115095.

10] Based on their structure, CNTs can be classified into two general categories: single walled (SWNTs), which consist of one layer of cylinder graphene and multi-walled (MWNTs), which contain several concentric graphene sheets

11] Shin B, Mondal S, Lee M, Kim S, Huh YI, Nah C. Flexible thermoplastic polyurethane-carbon nanotube composites for electromagnetic interference shielding and thermal management. Chemical Engineering Journal. 2021 Aug 15;418:129282.

12] Anzar N, Hasan R, Tyagi M, Yadav N, Narang J. Carbon nanotube-A review on Synthesis, Properties and plethora of applications in the field of biomedical science. Sensors International. 2020 Jan 1;1:100003.

13] Reed N, Balega J, Barwick T, Buckley L, Burton K, Eminowicz G, Forrest J, Ganesan R, Harrand R, Holland C, Howe T. British Gynaecological Cancer Society (BGCS) cervical cancer guidelines: recommendations for practice. European Journal of Obstetrics & Gynecology and Reproductive Biology. 2021 Jan 1;256:433-65.

[14] N.W.S. Kam, M. O'Connell, J.A. Wisdom, et al., Carbon nanotubes as multifunctional biological transporters and near-infrared agents for selective cancer cell destruction, Proc. Natl. Acad. Sci. 102 (2005) 11600–11605.

15] Ashikbayeva Z, Tosi D, Balmassov D, Schena E, Saccomandi P, Inglezakis V. Application of nanoparticles and nanomaterials in thermal ablation therapy of cancer. Nanomaterials. 2019 Aug 24;9(9):1195.

16] Cai Y, Wei Z, Song C, Tang C, Han W, Dong X. Optical nano-agents in the second near-infrared window for biomedical applications. Chemical Society Reviews. 2019;48(1):22-37.

18] Young JK, Figueroa ER, Drezek RA. Tunable nanostructures as photothermal theranostic agents. Annals of biomedical engineering. 2012 Feb;40:438-59.

19] Mitchell MJ, Billingsley MM, Haley RM, Wechsler ME, Peppas NA, Langer R. Engineering precision nanoparticles for drug delivery. Nature Reviews Drug Discovery. 2021 Feb;20(2):101-24.